Optics Communications 427 (2018) 557–562

Contents lists available at ScienceDirect

Optics Communications

journal homepage: www.elsevier.com/locate/optcom

Surface profilometry using vortex beams generated with a spatial light modulator

Alejandra Serrano-Trujillo [a], Matthew E. Anderson [b,*]

[a] Universidad Autonoma de Baja California, Tijuana, Baja California, 22390, Mexico
[b] Department of Physics, San Diego State University, San Diego, CA 92182, USA

ARTICLE INFO

Keywords:
Spatial light modulators
Optical vortices
Profilometry

ABSTRACT

We present a common path interference setup for detection of surface depth differences of the order of 200 nm, using a vortex and a Gaussian beam generated with a spatial light modulator. The phase of a vortex with a topological charge +1 and the phase of a lens are encoded next to each other onto the spatial light modulator. Both beams are incident onto a surface with a step feature; the Gaussian beam is incident onto a flat mirrored surface, while the vortex beam scans through the step. Upon interaction with the testing surface, both beams are superposed and their interference pattern is captured, collecting a set of images as a result of the scanning process. A phase detection algorithm is applied to these images and by tracking the vertical positions of the phase singularity along the scanning, the depth variations are estimated. The proposed set up is able to detect a 179 nm step feature, working with light at a wavelength of 830 nm and using a vortex with a diameter of 177 μm.

1. Introduction

The generation, propagation and application of optical vortices have turned these phase singularities into a subject with great research interest over the last few decades. Different techniques have been proposed for the generation of these beams; such as interferometric setups [1], segmented deformable mirrors [2], use of spiral phase plates [3], liquid crystal cells [4], or in general, the use of birefringent elements [5]. The use of a specific element for the vortex generation depends on the requirements of the application under study. Common applications found are related to the use of vortices for optical trapping [6], as waveguides [7] for quantum entanglement [8] and for microscopy [9,10].

The use of optical vortices for microscopy represents a profilometry application that attracts attention regarding how optical vortices can improve sensing on both conventional and new microscopy techniques. Several approaches in this field have been reported, for example, involving phase contrast microscopy, in one shot [9] and involving interferometry, through scanning [10]. It has been shown that a vortex beam enables edge detection with resolutions exceeding the diffraction limit of classical optical microscopic imaging systems [11], leading to a broad study of the superresolution effects produced by optical vortices. These studies have indicated that interferometric vortex localization methods are more accurate than methods based on the intensity pattern inspection [10].

A conventional interferometry approach using a pair of Gaussian beams offers high resolution measurements [12] by tracking the position of the fringes within an interference pattern. The shift of the fringes indicates an optical path difference between both Gaussian beams, interpreted as differences between the surfaces under test. The correct interpretation of this shift depends on the distance between the scanned areas, on the algorithm that tracks the fringes and, in certain configurations, it relies as well on the atmospheric conditions that may shift the fringes or alter the stability of the interferometer. Therefore, it is of interest to implement a technique with stability for interferometric measurements, that relies on the extracted phase from an interferogram rather than on counting fringes. A proposal with this characteristics would represent a simple and robust optical setup for microscopy applications.

In this work, we propose the use of a spatial light modulator (SLM) for the generation of Gaussian and vortex beams, manipulating their positions and allowing their interference upon reflection from the testing object. With this, we exploit the SLM as a dynamic device, simplifying the generation and shift of a vortex through code, keeping a common path between both beams and allowing their stable interference.

In Section 2, the experimental setup, the surface of the height feature acquired, the scanning process and the phase detection are described. In Section 3, the results from the experiments over a flat surface and over the height feature are presented, a coefficient of variation is computed

* Corresponding author.
E-mail address: manderson@sdsu.edu (M.E. Anderson).

https://doi.org/10.1016/j.optcom.2018.07.003
Received 17 April 2018; Received in revised form 12 June 2018; Accepted 1 July 2018
Available online 5 July 2018

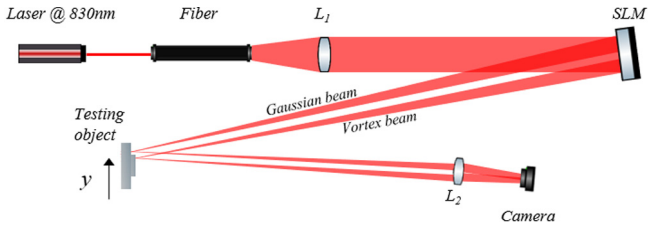

Fig. 1. Experimental setup for surface scanning by interference of a Gaussian and a vortex beam. The interference of a pair of beams modulated by the SLM allows the height measurement of a reflective testing object.

for analysis, and the estimated height and lateral dimensions of the structure are presented. Finally, in Section 4, our conclusions are listed, proving that a vortex with a 177 μm diameter is able to detect a step of 179 nm.

2. Experimental conditions

Experimental setup. The experimental setup is depicted in Fig. 1. A 830 nm light beam emitted by a 60 mW laser diode is coupled into a fiber, that acts as a spatial filter and delivers a clean Gaussian beam to the collimation lens L_1. The collimated beam is incident onto the SLM, where two patterns have been encoded; the phase of a lens and the phase of a vortex with a topological charge +1. Upon reflection from the SLM, both beams propagate, and as indicated in Fig. 1, a focused Gaussian beam interacts with a flat mirrored surface while a focused vortex beam scans across the step feature. Both objects are located on a translation stage that is shifted in the y direction. As previously analyzed [13], the vortex beam is highly sensitive to surface depth variations, affecting its structure upon interaction. Upon reflection from the object, the split vortex and the Gaussian beam traverse lens L_2 and overlap forming a fringe pattern on the beam profiling camera.

Generation of beams. The SLM in use is a Hamamatsu X8267, a liquid crystal on silicon reflection type modulator with an active area of 1024 × 768 pixels, covering 20 × 20 mm^2. The patterns presented in Fig. 2(a) and (c) show the phase of lenses with a constant diameter of 250 pixels, and the phase of vortices with a topological charge +1, with a diameter of 510 and 440 pixels, respectively. Notice that both Fig. 2(a) and 2(c) present patterns with the same focal length, but limited by a different diameter. Fig. 2(b) shows the intensity of the beams produced from the patterns in Fig. 2(a), demonstrating that a large numerical aperture, in this case a diameter of 510 pixels, results in a tight focusing spot of 177 μm. Fig. 2(d) shows the intensity of the beams produced from the patterns in Fig. 2(c), demonstrating that a smaller numerical aperture, in this case a diameter of 440 pixels, results in a loose focusing spot of 220 μm. Given the array of pixels available in the modulator, and avoiding the usage of additional optical elements for focusing, the vortex from Fig. 2(b) is the smallest achieved in this proposal. These characteristics are achieved by manipulating through a software algorithm the phase of the patterns displayed onto the SLM, modifying the spiral phase and the focal length of a vortex and a Fresnel lens. This algorithm is implemented in LabVIEW, allowing a more dynamic usage of the SLM, since any modification applied to the phase pattern is immediately displayed. The position of the beams is manipulated by adding as well the phase of a blazed grating, and the size of each focused spot is determined by the resolution, in pixels, of the pattern encoded onto the SLM, as presented in Fig. 2. The distribution of the patterns displayed over the SLM in Fig. 2 represents a similar approach with respect to the SLM calibration process proposed by Zhang H. et al. [14].

The phase patterns encoded onto the SLM are located close to each other, hence, both beams travel nearly the same distance, allowing their interference in this setup. The pair of beams will interact upon reflection from a flat surface and a calibration standard, presented in Fig. 3.

Testing object. The testing object consists of a Nanuler calibration standard with a step height feature of a dog bone structure 2 mm long and 500 μm wide [15]. The height feature consists of thermally grown SiO_2 coated in chrome, and represents a reflective and uniform difference of 179 nm with respect to the surrounding surface. In Fig. 3(a) a diagram offered by the manufacturer of the calibration standard is presented [15], where the location of the calibration structure has been highlighted. This calibration standard was mounted onto a flat mirror with a drop of RTV silicon adhesive, as presented in Fig. 3(b), in order to have a flat reference for the Gaussian beam. Notice that in Fig. 3(b), the location of the height feature is highlighted as well, and the material surrounding the calibration standard is the flat mirror. The squared structures of the height feature are 500 μm wide, while the rectangular structure from the middle is 1 mm long and 200 μm wide. These dimensions indicate that, in order to scan the thin feature, a vortex with a diameter less than 200 μm should be used, while a vortex with larger diameter can be used for scanning the 500 μm wide areas. Therefore, the 177 μm vortex is used for scanning over the thin feature of the calibration structure, while the 220 μm vortex is used for scanning over the 500 μm wide feature. In both cases, the Gaussian beam scans over the mirror, considered as a flat reference with a $\lambda/10$ surface flatness. Interference fringes are obtained from this experiment. These interferograms are captured as images of 512 × 512 pixels, using a WinCamD UHR, an IR beam profiling camera with a working area of 6.6 × 5.3 mm^2.

Scanning process. The location of each beam during this experiment is presented in Fig. 4. The lines in Fig. 4 indicate the path followed by the vortex beam through the structure, while the Gaussian beam follows a reference path over the mirror. Path $Scan_A$ and path $Scan_D$, indicated with dashed lines, are followed using the vortex beam of diameter of 220 μm, while $Scan_B$ and $Scan_C$, indicated with dotted lines, are the paths followed using the vortex beam of diameter of 177 μm. As described in Fig. 1, the testing object is located on a translation mount, with the step horizontally aligned, therefore, the y direction of the mount is vertical. For every vertical shift, a fringe pattern is captured and stored for analysis. The scanning process generates a set of images and a phase detection algorithm is applied to every image within this set. The phase detection algorithm adopted in this work was proposed by Takeda et al. [16], which is based in the filtering of the carrier frequency contained within an interferogram. Fig. 5 shows an example of this phase detection process.

Phase detection algorithm. The false color interferogram from Fig. 5 shows the characteristic fork of a vortex, indicating its presence. This fringe pattern is mapped to the spatial frequency domain via 2D FFT, where the first order component is filtered. Then, the data is mapped back to the spatial domain via inverse 2D FFT. A wrapped phase map is found, where the grayscale, ranging from black to white, indicates phase values from $-\pi$ to π. A phase singularity is seen in this spatial domain map, indicating the vortex position [10]. Similarly to the interpretation of an interference experiment involving two Gaussian beams; where a shift of the fringes indicates an optical path difference between the beams, a shift in the position of the vortex singularity within the spiral phase pattern indicates an optical path difference with respect to a previous position. Considering that the scanning process described in Fig. 4 collects a set of interferograms, this approach proposes to extract the phase and to track the position of the singularity over the complete set. Information regarding the height of the testing object is recovered from this analysis.

3. Analysis of results

In order to verify this approach, the scanning process described in Section 2 was carried out for a flat surface (mirror) with no testing object. Fig. 6 shows the position of the vortex singularity for this